Scilight

Journal of Mechanical Engineering and Manufacturing

https://www.sciltp.com/journals/jmem

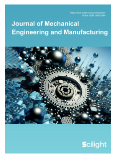

Review

Check for updates

Design and Manufacture of Devices for the Testing of Adhesives and Adhesive Joints

André F. V. Pedroso [1,2,*], Arnaldo G. Pinto [1], Paulo J. R. O. Nóvoa [1,3], Rui M. Fazenda [1], José G. F. Barbosa [1], Diogo A. M. Solha [1] and Isabel M. Pinto [1,4]

[1] CIDEM, ISEP, Polytechnic of Porto, Rua Dr. António Bernardino de Almeida, 4249-015 Porto, Portugal
[2] Department of Mechanical Engineering, Faculty of Engineering, University of Porto, Rua Dr Roberto Frias, 400, 4200-465 Porto, Portugal
[3] Associate Laboratory for Energy, Transports and Aerospace (LAETA-INEGI), Rua Dr Roberto Frias, 400, 4200-465 Porto, Portugal
[4] LEMA, ISEP, Polytechnic of Porto, Rua Dr. António Bernardino de Almeida, 4249-015 Porto, Portugal
* Correspondence: afvpe@isep.ipp.pt; Tel.: +351-228340500

How To Cite: Pedroso, A.F.V.; Pinto, A.G.; Nóvoa, P.J.R.O.; et al. Design and Manufacture of Devices for the Testing of Adhesives and Adhesive Joints. *Journal of Mechanical Engineering and Manufacturing* **2026**. https://doi.org/10.53941/jmem.2026.100025

Received: 23 March 2026
Revised: 17 April 2026
Accepted: 12 May 2026
Published: 5 June 2026

Abstract: The reliability of mechanical testing of adhesive joints is strongly dependent on the design and performance of the testing fixtures, jigs or apparatus used to manufacture and load the specimens. Inadequate devices design may introduce misalignment, parasitic stresses, and uncontrolled adhesive thickness, compromising the accuracy and repeatability of experimental results. This paper presents the design, development, and manufacture of a set of dedicated mechanical devices for the characterisation of adhesive joints, specifically targeting floating roller peel and butt-joint tensile testing. These devices will ensure that the testing laboratory is duly equipped and qualified to carry out the specified tests for both research activities and industrial applications. The proposed system comprises three main components: a floating roller peel fixture compliant with ASTM D3167, a modular jig for the fabrication of butt-joint specimens with controlled adhesive thickness, and a self-aligning apparatus for tensile testing of butt joints. The design process was guided by key mechanical requirements, including precise load alignment, minimisation of frictional effects, controlled kinematics, and robustness under repeated testing conditions. All components were developed using CAD modelling and manufactured through precision machining using structural steels and aluminium alloys. Particular attention was given to the control of geometric tolerances, alignment mechanisms, and load transfer paths, ensuring consistent specimen positioning and minimisation of secondary stresses during testing. The proposed devices provide a versatile and cost-effective solution for laboratory-scale mechanical testing, enabling improved repeatability and reliability of experimental procedures. Experimental validation was performed using epoxy and polyurethane adhesives with distinct mechanical properties, which experimental values are addressed in another paper. Overall, the presented design contributes to the standardisation and optimisation of experimental methodologies for adhesive joint characterisation, supporting more accurate and reproducible mechanical testing in engineering applications.

Keywords: adhesive joints; tool design; mechanical testing devices; alignment control; experimental setup; floating roller peel test; butt-joint testing

1. Introduction

The design of mechanical testing systems represents a fundamental link between theoretical models of material behaviour and the experimental methods employed to validate them [1]. In the field of adhesive bonding, this link assumes particular importance, as the mechanical response of bonded joints is highly sensitive to the manner in which loads are introduced, transmitted, and constrained [2]. Consequently, the reliability of experimental characterisation depends not only on the intrinsic properties of the adhesive and substrates, but also on the mechanical integrity, geometric accuracy, and kinematic performance of the testing apparatus [3].

Adhesive joints are increasingly used in structural applications across a wide range of industries, including aerospace [4,5], automotive [6,7], marine [8,9], and civil engineering [10,11], owing to their ability to join dissimilar materials, improve stress distribution, and reduce structural weight [12]. However, these advantages are accompanied by complex and often non-linear mechanical behaviour that arises from the heterogeneous nature of bonded interfaces and the viscoelastic and plastic characteristics of modern structural adhesives [13]. Monajati et al. [14] comprehensively reviewed the tensile behaviour of adhesively bonded joints, highlighting the influence of joint configurations, failure mechanisms, and modelling strategies, and providing design-oriented insights into how geometry, materials, and simulation methods govern strength, damage tolerance, and structural efficiency. Accurate experimental assessment of joint performance is therefore essential for both design validation and the development of predictive numerical models [15]. This requirement places stringent demands on the design of mechanical testing systems, which must ensure that the imposed loading conditions closely conform to the assumptions embedded within analytical and standardised test methodologies [16]. Figure 1 presents a conceptual overview of adhesively bonded joints, highlighting the interdependence between materials, joint configuration, surface preparation, and loading conditions, all of which must be consistently reproduced during experimental testing.

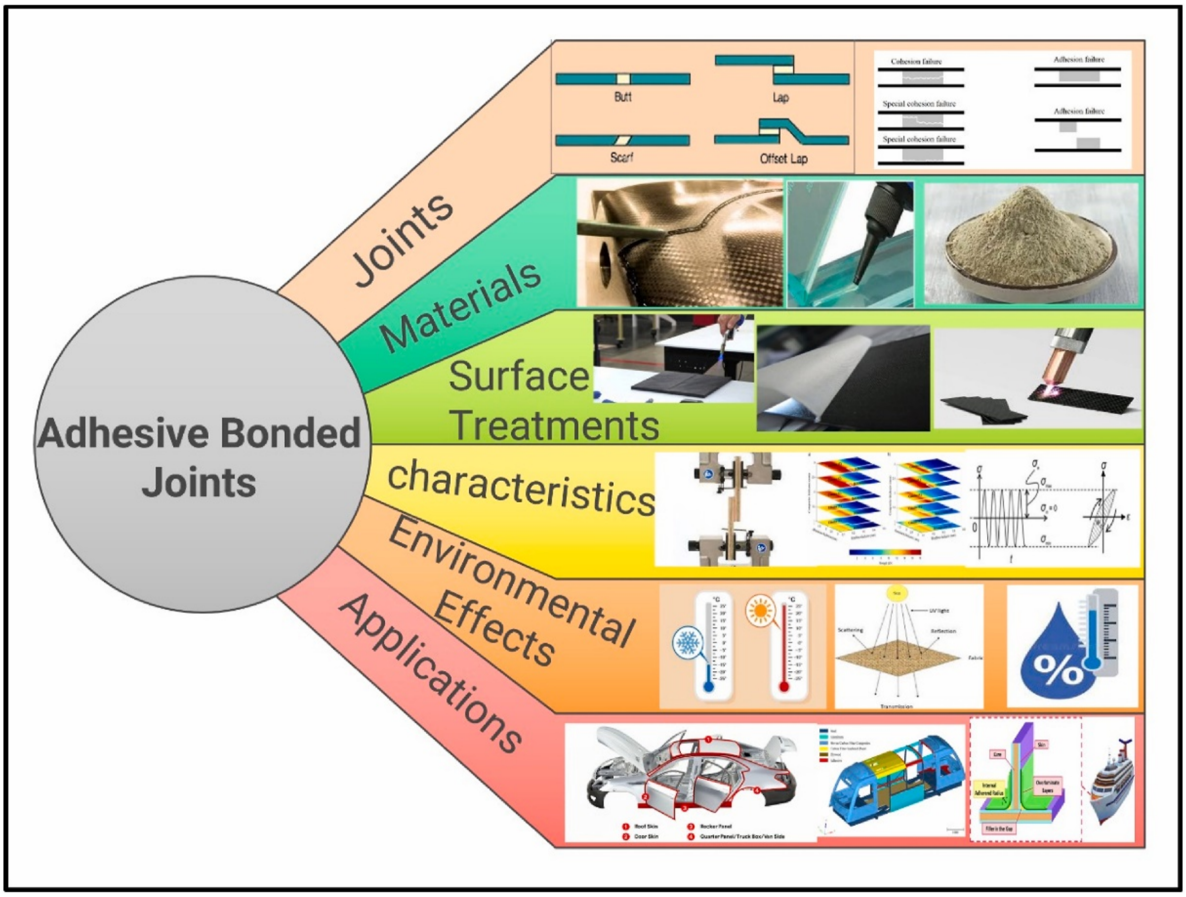

Figure 1. Schematic overview of the principal domains governing the behaviour and performance of adhesively bonded joints, highlighting the interrelated roles of joint configuration, constituent materials, surface treatments, mechanical characteristics, environmental effects, and engineering applications [17].

In this context, the accuracy and repeatability of experimental results are strongly influenced by the design of the devices used for specimen fabrication and testing. Inadequately designed devices may introduce parasitic effects, including misalignment, frictional resistance, and unintended bending or torsional moments, which can significantly distort the measured response and compromise the comparability of results across different laboratories [3]. Unlike conventional testing of bulk materials, adhesive joint testing requires careful control of both specimen geometry and load introduction, placing additional demands on tool design.

A critical aspect of experimental characterisation is the control of adhesive layer thickness and the alignment of the adherends during specimen fabrication. Variations in bond-line thickness can significantly affect stiffness, strength, and failure mechanisms, constituting a major source of experimental scatter. Therefore, fabrication jigs must ensure precise positioning, allow fine adjustment of the interfacial gap, and provide access for adhesive application and removal of excess material, while maintaining structural rigidity and dimensional stability [18]. These requirements highlight the need to consider fabrication and testing tools as integral components of the experimental system rather than auxiliary elements.

The importance of jigs and fixtures in ensuring positional accuracy and process repeatability is well established in manufacturing engineering. Figure 2 illustrates typical jig and fixture configurations, including locating elements, clamping systems, and guiding features, which constrain the workpiece and control its degrees of freedom during processing. In adhesive joint testing, similar principles apply, but with additional constraints related to load alignment, minimisation of parasitic effects, and control of adhesive geometry. Systematic studies identify alignment control, structural stiffness, and functional modularity as key drivers in fixture design Fiedler et al. [19].

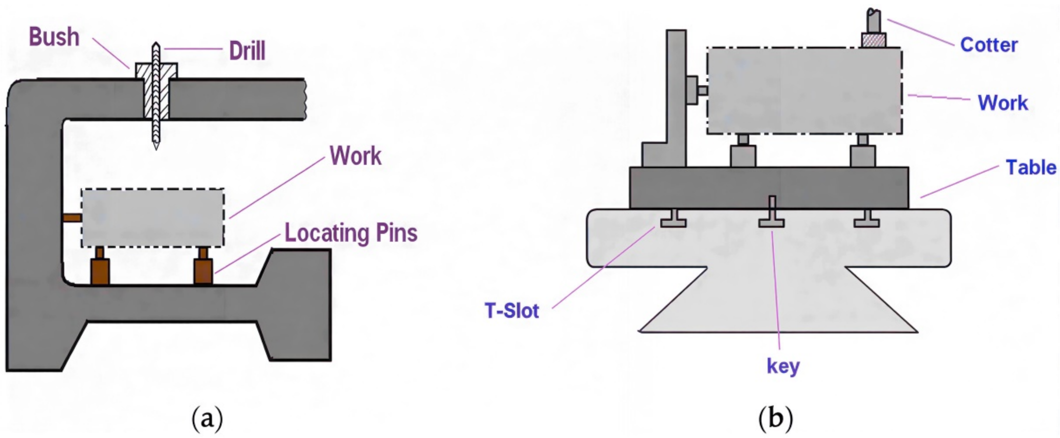

Figure 2. Representative examples of (**a**) a drilling jig and (**b**) a machining fixture [20].

While the testing of monolithic specimens typically involves relatively simple boundary conditions and well-defined stress states, bonded assemblies are characterised by highly localised stress gradients and a strong coupling between normal and shear components at the adhesive layer. ASTM D897 [21] standard prescribes a butt-joint configuration whose valid implementation inherently requires the use of precision bonding tools to ensure strict parallelism between adherends, together with self-aligning testing fixtures to minimise bending and secondary stresses. Although the standard does not define a specific jig geometry, it establishes stringent geometric and loading requirements that strongly govern jig and fixture design. In Van Massenhove et al. [22] study, a bespoke concentric PTFE jig ensured accurate axial alignment and controlled bond-line thickness, enabling radial adhesive injection that limited air entrapment and improved the reproducibility of viscoelastic butt-joint fabrication. Zhang et al. [23] used a custom mould to fabricate butt-joints, incorporating a V-groove alignment system, a locating ring and a top-screw pressing mechanism to ensure high coaxiality, controlled 1 mm bond-line thickness, and reproducible hollow cylindrical specimens for cyclic testing. Also, Mu et al. [24] employed an in-house-made butt-joint jig and fixture providing concentric positioning, rigid axial constraint and controlled bond-line thickness via calibrated spacers, enabling reproducible fabrication and minimisation of eccentricity-induced secondary stresses during subsequent mechanical testing.

Regarding the testing apparatus, Wahab et al. [25] utilised a butt-joint fixture derived from an ASTM STP (Special Technical Publication), incorporating specialised upper and lower grips to ensure accurate axial loading, controlled adhesive confinement, and consistent stress states suitable for triaxiality-oriented mechanical assessment. The geometry and stiffness of the fixture, the alignment of the load path, and the compliance of connecting elements all exert a direct influence on the resulting stress distribution within the joint. Consequently, the design of testing machinery must adopt a systems-based approach, in which the specimen, the fixture, and the testing machine are considered as an integrated mechanical assembly rather than as independent components [26].

One of the principal challenges in the design of adhesive testing devices lies in achieving and maintaining precise alignment throughout the loading process. Even minor angular or translational misalignments can introduce secondary bending moments that alter the effective loading mode, particularly in tensile and peel configurations. These effects have been well documented in the literature, where misalignment–induced bending has been shown to alter effective stress states and failure loads in tensile and peel tests, and are discussed in classic texts on adhesive joint behaviour [27]. To mitigate these issues, machine designers must incorporate kinematic features that allow for self-alignment or controlled degrees of freedom (DOF), while simultaneously ensuring sufficient structural rigidity to prevent excessive deformation under load. The selection and placement of bearings, pins, and guiding surfaces thus become critical elements of the overall design strategy [28].

In peel and debonding tests, such as the floating roller peel test, additional complexities arise from the need to minimise friction and maintain a constant and well-defined peel angle. The presence of rolling elements introduces dynamic interactions between the fixture and the specimen, requiring careful consideration of contact mechanics, bearing tolerances, and surface finishes [29]. The machine design must ensure that the motion of the roller is governed primarily by the applied load rather than by parasitic resistances, as even small frictional forces can lead to significant errors in the measured peel force, particularly for flexible substrates and low-strength adhesive systems [30]. This necessitates the integration of high-precision rolling bearings and accurately machined components, as well as the adoption of appropriate materials and surface treatments to enhance wear resistance and dimensional stability.

Within this framework, the development of robust, standard-compliant, and reproducible testing fixtures becomes essential to ensure reliable experimental characterisation. Despite this need, detailed descriptions of fixture design methodologies, including loading path definition, alignment strategies, tolerance control, and manufacturing considerations, remain limited in the literature. This creates a need for documented, transparent, and reproducible design methodologies that can be adopted or adapted by other researchers and practitioners.

The present work addresses this gap by presenting the design, development, and manufacture of a set of dedicated mechanical devices for the characterisation of adhesive joints. The proposed devices comprises a floating roller peel fixture compliant with ASTM D3167 [31] standard, together with an original in-house jig for the fabrication of butt-joint specimens and a custom-designed apparatus for their tensile testing in accordance with ASTM D897 [21] and ASTM D2095 [32] standards. The design approach is guided by key machine design principles, including alignment control, minimisation of parasitic effects, definition of kinematic constraints, and structural robustness. The present manuscript aims to describe the main features and capabilities of these devices.

The manuscript is organised as follows. Section 1 presents the theoretical background together with a comprehensive review of the relevant literature. Section 2 describes the design and manufacture of the floating-roller peel fixture, the butt-joint fabrication jig, and the dedicated tensile-testing apparatus. This section also reports the cost associated with each device. Section 3 discusses the characteristics and cost values of the developed devices. Finally, Section 4 summarises the principal conclusions, and Section 5 outlines future considerations and potential developments aimed at enhancing specific design features and extending the capabilities of the proposed testing systems.

2. Materials and Methods—Fixture, Jig and Apparatus

This section introduces the design and manufacturing of the mechanical devices developed for adhesive testing. The presented solutions address both specimen fabrication and mechanical loading, with emphasis on alignment accuracy, adhesive thickness control, and standard compliance. The following subsections describe in detail the floating roller peel fixture, the butt-joint fabrication jig, and the dedicated tensile testing apparatus, highlighting their design rationale, manufacturing processes, functional characteristics, and associated production costs.

2.1. Fixture Design and Manufacturing for the Floating Roller Peel Test

The floating roller peel test fixture was developed in accordance with the requirements of ASTM D3167 standard [31]. The design was guided by three main mechanical requirements: minimisation of frictional resistance, maintenance of stable specimen alignment during testing, and prevention of parasitic contact between rotating and stationary components. Figure 3 presents the assembly drawing of the fixture, generated using SolidWorks®. For clarity, the screws securing the side plates to the shafts are not shown.

The alignment of the fixture is ensured by the symmetric lateral plates and by the use of matched mounting holes on both sides of the assembly, which keep the roller shafts parallel and the rollers properly positioned within the same plane. The bearing-supported roller arrangement promotes concentric rotation and stable guidance of the peeled arm, while the geometry of the side plates preserves the relative position between the machine connection point and the roller set. This layout helps maintain a consistent peel path and minimises misalignment-induced parasitic effects during testing.

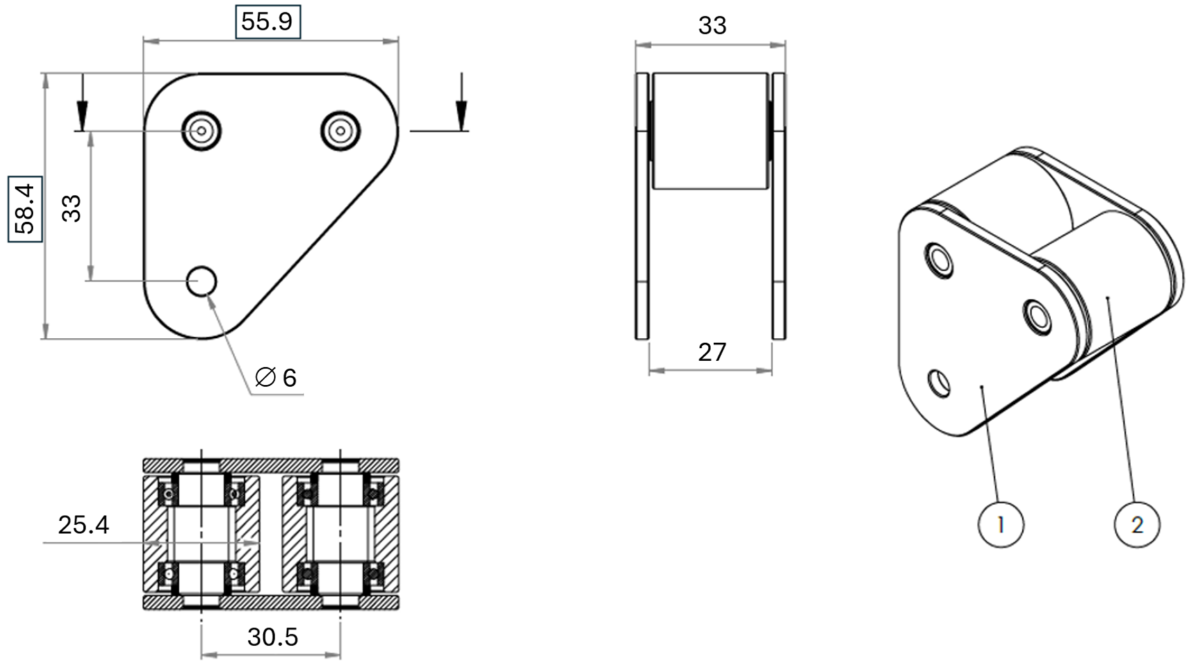

Figure 3. General assembly drawing of the floating roller peel testing apparatus.

Figure 4 illustrates the fixture in a partially assembled state, with one of the rollers is already mounted with its corresponding shaft and bearings. The fixture consists of two lateral plates (1), each with a thickness (t) of 3 mm and three openings. One of these openings, with a diameter ($Ø$) of 6 mm, accommodates the pin used to connect the fixture to the testing machine. The other two openings, with a $Ø$ = 8 mm, are used to mount the rollers (2), each measuring $Ø$ = 25.4 mm and 25.4 mm in length (L). The rollers are hollow to accommodate the shaft–bearing assembly and to ensure smooth rotation under loading. The rollers are hollow to allow passage of their respective shafts (3).

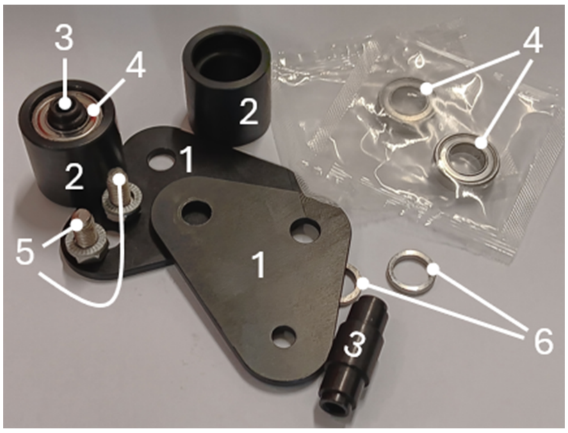

Figure 4. Partially assembled floating roller peel testing apparatus.

The inner diameter of each roller is 15 mm over a central length of 12.5 mm, while the adjacent end regions have an internal diameter of 19 mm, with tolerances selected to match the outer diameter of SKF 61800 bearings (4). The shaft ends have a diameter of 8 mm, corresponding to the openings in the lateral plates, and include threaded holes for fastening the assembly with M6×12 hexagonal head screws (5). The intermediate shaft sections have a diameter of 10 mm, dimensioned to fit the bearing bores, whereas the central shaft section has a diameter of 12 mm over a length of 12.5 mm. To prevent contact between the lateral plates and the roller ends, and thus avoid parasitic friction that could affect the measured peel force, spacer rings (6) were introduced. These rings have an external diameter of 13 mm, an internal diameter of 10 mm, and a thickness of 2 mm, providing a clearance of 0.8 mm between each lateral plate and the adjacent roller end. Nord-Lock washers were employed in the bolted connections to reduce the risk of loosening during repeated use. These washers are shown in the screws depicted in Figure 4. Figure 5a presents the fully assembled fixture, while Figure 5b shows the apparatus mounted on the tensile testing machine.

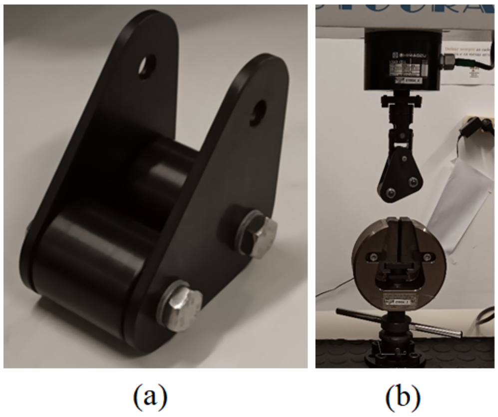

Figure 5. (**a**) Fully assembled floating roller peel testing apparatus; (**b**) Apparatus installed on the universal testing machine.

The principal load-bearing elements of the fixture are the lateral plates, shafts, connecting pin, and bolted joints, whereas the rollers and bearings primarily ensure guided motion and minimise parasitic friction during the test. The fixture was designed for the specimen configuration prescribed in ASTM D3167, and the admissible specimen thickness is therefore governed by the specimen geometry defined in that standard. For clarity, the geometry and dimensions of the peel specimen were not repeated here, as they are established by the applicable ASTM procedure.

As no prior in-house fixture with the same configuration was available, a direct quantitative comparison of friction reduction relative to an original device was not possible. Nevertheless, parasitic friction was minimized by design using rolling bearings, accurately machined shafts and rollers, and spacer rings providing 0.8 mm clearance between the lateral plates and the roller ends, thereby preventing unintended contact. In addition, the floating-roller configuration was adopted to maintain stable peel geometry during testing. Although a separate quantitative calibration of friction torque and peel-angle deviation was not carried out in the present study, these aspects were addressed through the mechanical design of the fixture and should be considered in future calibration work.

All components of the fixture, namely the lateral plates, rollers, shafts, and spacer rings, were manufactured by machining. The shafts were manufactured from FR3 steel (DIN: 34CrNiMo6), a heat-treated alloy steel selected for its superior mechanical performance relative to conventional carbon steels, particularly in terms of strength and durability. The remaining components were fabricated from CK45 steel. With the exception of the spacer rings, all machined parts were treated with a black oxide finish to improve surface protection. All manufactured parts, together with additional components such as bearings, screws, and washers, were supplied by the company responsible for producing the fixture, and the total cost was estimated at approximately €400, as detailed in Table 1.

Table 1. Indicative cost of the floating roller apparatus at the time of manufacture.

Component	Quantity	Cost (nº of Pieces × Unit Cost)
Sheet metal (1) *	2	2 × €85 = €170
Rolling elements (2) *	2	2 × €70 = €140
Threaded shaft (3) *	2	2 × €25 = €50
SKF 61800 roller bearing (4) *	4	4 × €10 = €40
ISO 4014 M6×12 bolt with Nord-lock washers (5) *	4 + 4	**
Spacing rings (6) *	4	**
Total	22	€400

* regarding Figure 4 numbers. ** price is irrelevant, considering the remaining components.

It should be noted that this type of fixture is commercially available from several suppliers of mechanical testing equipment. However, at the time of the present analysis, the estimated acquisition cost of commercial alternatives was found to be substantially higher than the indicative manufacturing cost reported into Table 1.

It should be emphasised that the scientific contribution of the present fixture does not reside solely in its compliance with ASTM D3167, but in the explicit engineering solutions adopted to control parasitic effects that are not prescribed in detail by the standard. In particular, the apparatus combines a bearing-supported roller arrangement, a symmetric side-plate architecture, and a controlled 0.8 mm clearance between the roller ends and the lateral plates, obtained through spacer rings, in order to minimise frictional interference and preserve a stable peel path during testing. These features constitute the main original aspects of the proposed design, together with its comparatively low indicative manufacturing cost of approximately €400, which supports its practical implementation in laboratory environments.

2.2. Design and Manufacture of a Jig for Butt Joint Fabrication

The butt-joint tensile test involves the application of a longitudinal force to a butt joint until failure of the adhesive layer occurs. Two ASTM standards may be applied: ASTM D897 [21], which employs short circular substrates manufactured from metal or wood, and ASTM D2095 [32], which encompasses both circular and square geometries.

For the fabrication of butt-joints, the use of dedicated jigs is essential to ensure accurate substrate alignment and consistent adhesive thickness. The jig, which is illustrated in the Figure 6 was developed within the scope of this work was required to meet the following specifications:

- Ensure accurate alignment of the substrates.
- Allow controlled adjustment of the adhesive thickness.
- Provide full access to the bonding perimeter for removal of excess adhesive prior to curing.
- Enable adhesive curing both at room temperature and at elevated temperatures (up to approximately 120 °C).
- Allow the preparation of at least five butt-joint specimens simultaneously.
- Accommodate cylindrical substrates with a diameter of 12.7 mm and a length of 40 mm, allowing flexibility for other dimensions.
- Ensure ease of handling and mobility of the jig.

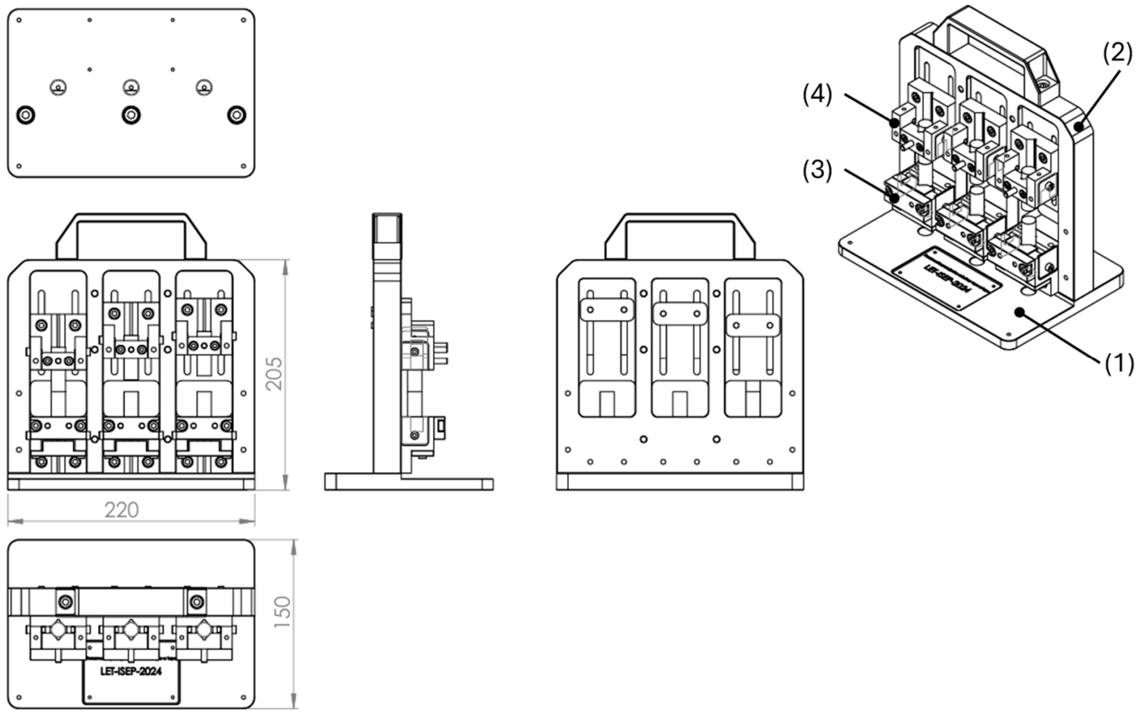

Figure 6. Engineering drawing of the jig designed for the fabrication of butt-joint specimens.

The jig can be divided into four main components: the base (1), the vertical plate (2), the lower support (3), and the upper support (4). In the assembly shown in Figure 6, the handle (Elesa M.443-140-CH) fixed at the top of the vertical plate and the cylindrical substrates mounted between the lower and upper supports can also be observed. It is noteworthy that two identical jigs were developed, allowing the fabrication of six butt-joints in total. This configuration, based on two jigs capable of producing three joints each, was preferred over a single larger jig for six joints, in order to improve handling, reduce weight, and facilitate transport.

The base (1), manufactured from an aluminium alloy (AW 6082), allows the jig to be positioned on a workbench and provides support for securing the vertical plate using three M8×20 socket head cap screws. The maximum dimensions of the base are 220 × 150 × 15 mm^3.

The vertical plate (Figure 7), produced from CK45 steel, contains three vertical channels on its faces, designed to house the substrate supports. These channels ensure proper alignment of the supports, and consequently, of the substrates. At the lower ends of the channels (regions marked with (a) in Figure 7), the lower supports are fixed using two screws. Each channel also includes two vertical slots through which screws are inserted to secure the upper support (regions marked with (b) in Figure 7). The lower section of the channels is completely open, facilitating access to the butt-joint region closest to the vertical plate (regions marked with (c) in Figure 7). In cases of room-temperature curing, this opening enables the removal of excess adhesive around the entire joint perimeter. The top surface of the vertical plate includes two threaded holes for attaching a handle using M6×16 socket head cap screws, while the bottom surface includes three threaded holes for securing the plate to the base. The maximum dimensions of the vertical plate are 220 × 190 × 25 mm^3.

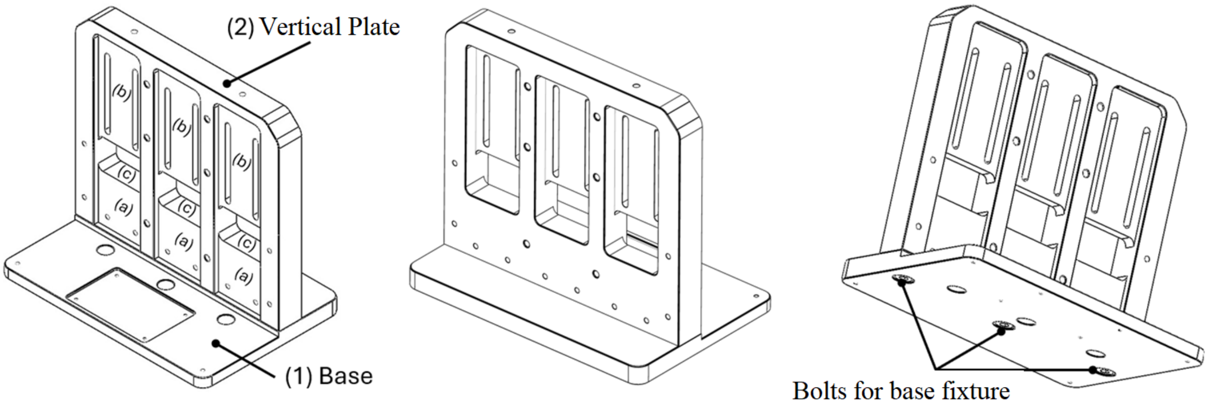

Figure 7. Assembly of the base plate and vertical support plate.

The lower and upper supports, shown in Figure 8, are composed of multiple components and functions to secure the substrates and ensure their correct positioning during fabrication.

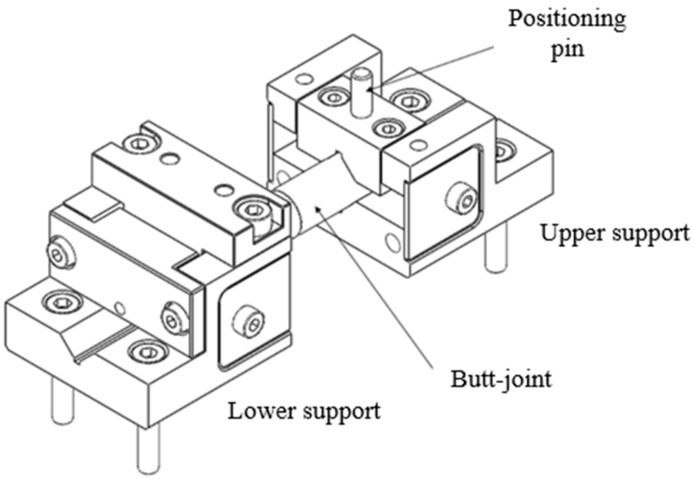

Figure 8. Assembly of the lower and upper support components.

The lower support (Figure 9) is positioned within the machined channels of the vertical plate and fastened using two M5×30 socket head cap screws. The substrate is clamped between two V-shaped surfaces (jaws) using M5×25 socket head cap screws, ensuring stable positioning and alignment. Although the use of positioning pins is not strictly necessary, they may be employed to define the orientation of the substrate hole axis, ensuring it remains parallel to the vertical plate. All components of the supports (both lower and upper) were manufactured by machining from aluminium alloy AW 6082, except for the lateral plates, which are fabricated from stainless steel (AISI 304) and laser-cut. These lateral plates, with a thickness of 1.5 mm, are not strictly necessary. However, during handling of the jig, they prevent the positioning pin from disengaging from the substrate hole. Stainless steel was used to manufacture these lateral plates, although other materials could also be used.

The upper support (Figure 10) is similarly composed of multiple components and serves to secure the upper substrate of the butt-joint. The supports are positioned within the machined channels on the face of the vertical plate, ensuring alignment with the lower supports. The method for clamping the substrate is identical to that of the lower support, with the substrate held between two V-shaped surfaces (jaws) using M4×25 socket head cap screws.

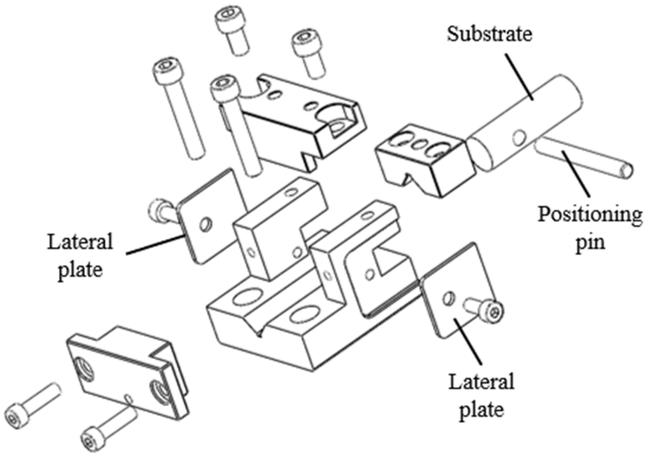

Figure 9. Exploded view of the lower support assembly.

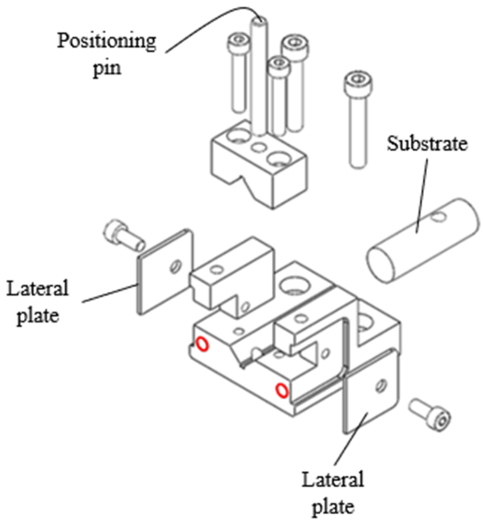

Figure 10. Exploded view of the upper support assembly.

Positioning pins may also be used in the upper support to define the orientation of the substrate hole axis, ensuring it remains perpendicular to the vertical plate. Substrates can be mounted without the pins; however, when both upper and lower pins are used, the axes of the substrate holes become orthogonal. During the butt-joint tensile test, the applied load is transmitted through the pins inserted into the substrate holes. Unlike the lower supports, the upper supports can be repositioned along the channels. Once the desired position is defined—corresponding to the intended adhesive thickness—they are fixed using M5×30 socket head cap screws passing through the slots and engaging plates housed in recesses at the rear of the vertical plate, as shown in Figure 11 (indicated in red). The gap between substrates directly defines the adhesive layer thickness.

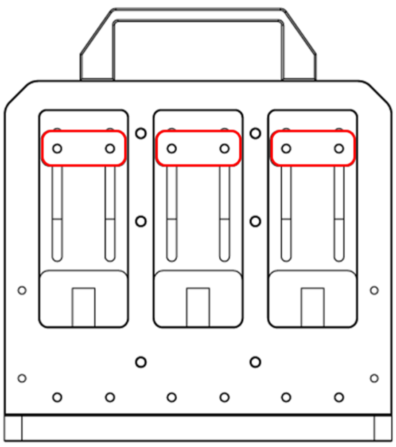

Figure 11. Rear view of the complete assembly.

The substrate supports includes two threaded holes at their tops (highlighted in red in Figure 10 for the upper support) for the insertion of M6 screws that function as mechanical stops, ensuring a controlled and repeatable gap between substrates and, consequently, controlling the adhesive thickness. Depending on the screw length, they may be installed in either one or both supports (upper and lower). The jig also allows the use of a transverse bar, fastened to the front of the vertical plate, as a stop for the upper supports. This feature will be discussed further below to clarify the function of stops, whether implemented as screws or as a bar.

Figures 12 and 13 presents images of the front and rear, respectively, of the jig developed and manufactured. As previously noted, two identical jigs were produced, allowing the fabrication of six butt-joints in total. The top two images show the front of the jigs, while the bottom two images display the rear. In the left-hand configuration, M6 screws are used as stops, whereas in the right-hand configuration, a steel bar serves as the stop for the upper supports, illustrating the flexibility of the design.

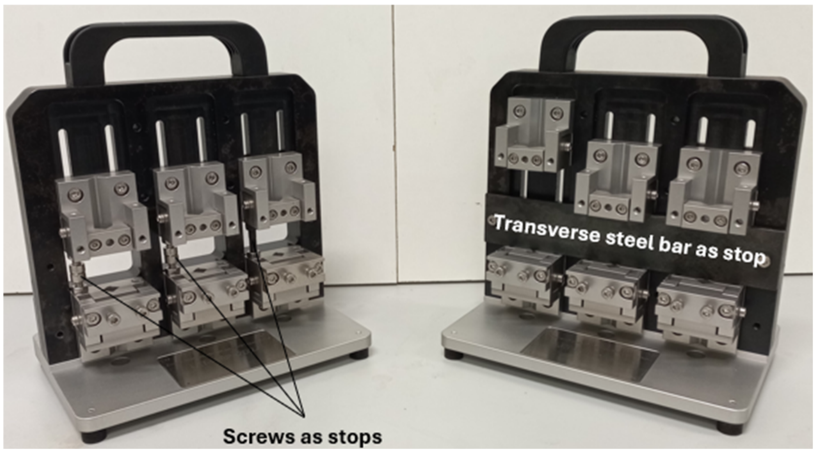

Figure 12. Front face of the assembled jig.

Figure 13. Rear face of the assembled jig.

The manufacture of butt joints using the proposed jig involves the stages illustrated in Figure 14, which are described in the following steps:

1. **Separate the upper support from the lower support.** Raise the upper support to an elevated position and secure it in place using the two M5×30 CHC screws (the lower support remains permanently fixed to the apparatus).
2. **Position and secure the lower substrate on the lower support.** Avoid contact with the bonding surface. A pin may be inserted into the hole of the substrate in order to ensure that its axis is approximately parallel to the vertical plate of the apparatus. Secure the lower substrate using the two M5×25 CHC screws.
3. **Position the upper substrate on the upper support.** Avoid contact with the bonding surface. As indicated in image (3) of Figure 14 a pin may be inserted through the hole in the clamp and the hole in the substrate. In this configuration, the axis of the hole is perpendicular to the vertical plate of the apparatus and, consequently, perpendicular to the axis of the hole in the lower substrate. Lightly tighten the substrate within

the clamps using the two M4×25 CHC screws, only to the extent necessary to prevent displacement under the action of gravity if the pin is not employed.

4. **Place a calibrated spacer plate on the surface of the lower substrate.** The plate must be suitably clean and must have the thickness corresponding to the desired adhesive layer thickness.
5. **Lower the upper support so that the upper substrate presses against the spacer plate.** Prior to this operation, loosen the two M5×30 CHC screws. If a pin has been inserted into the upper substrate, the stops should remain slightly disengaged and, in all cases, must be secured and free from play. However, if the pin referred to in step (3) has not been used, the support should be displaced as described in the subsequent step.
6. **Lower the upper support until its movement is arrested by the stops.** If a pin was inserted in step (3), it must be removed prior to this downward movement of the upper support. The upper substrate should not be excessively tightened within the clamps, as the clamps must be able to slide along the substrate during this downward motion.
7. **Secure the upper substrate within the clamps using the two M4×25 CHC screws.** During tightening, apply slight pressure to the upper substrate against the spacer plate and to the upper support against the vertical plate.
8. **Separate the upper support from the lower support.** Raise the upper support to an elevated position and secure it using the two M5×30 CHC screws.
9. **Apply the adhesive to the surface of the lower substrate.** The spacer plate must be removed prior to this operation.
10. **Lower the upper support until its movement is arrested by the stops** and secure its position using the M5×30 CHC screws. The adhesive layer thickness will be equal to the gap between the ends of the substrates, as previously defined by the spacer plate. In image (10) of Figure 14, the adhesive is not present.

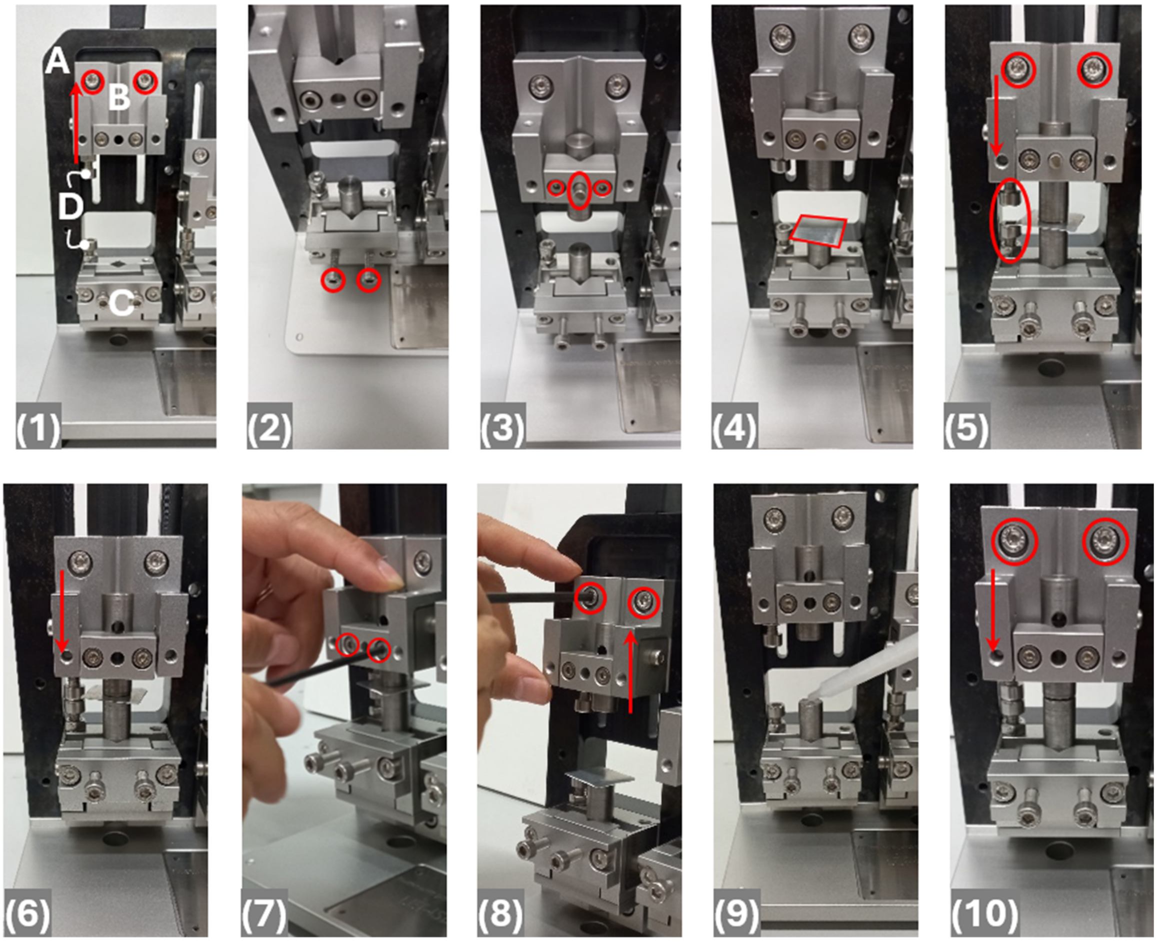

Figure 14. Procedural steps for the manufacture of butt joints using the developed jigs, A: Vertical plate; B: Upper support assembly; C: Lower support assembly; D: Mechanical stops.

The position of the screws acting as stops can be adjusted in height and is fixed using nuts. In Figure 14, the stops are located on the left side of the supports, although they can also be positioned on the right side. As shown in the left image of Figure 12, a steel bar can be used as a stop instead of screws. However, removal of the adhesive in the region closest to this bar is more difficult. In addition, the adhesive may come into contact with the bar; therefore, a release agent should be applied to its surface or a plastic film, such as PTFE, should be used.

As shown in Figure 15, the jig developed for butt joint manufacture ensures proper alignment (coaxiality) of the substrates and a uniform gap between them, thereby ensuring a consistent adhesive thickness. These constitute the main purposes of the jig.

Figure 15. Substrate alignment and interfacial gap.

In the present study, the required adhesive-layer thickness was defined by the calibrated spacer plate used during assembly and by the corresponding position of the mechanical stops, rather than by a universal fixed tolerance stated in the manuscript. Likewise, the alignment requirement was that the adherends remain coaxial during bonding to minimize eccentricity in the subsequent tensile test. These conditions were addressed using machined guide channels in the vertical plate and V-shaped clamping surfaces in the upper and lower supports. However, a separate metrological quantification of the achieved bond-line thickness accuracy, the residual specimen misalignment, and the gap variation caused by differential thermal expansion during elevated-temperature curing was not carried out in the present study. These aspects should therefore be regarded as important design considerations and limitations of the current jig, to be addressed in future calibration work.

When using adhesives prone to flow, it is necessary to place a small conical silicone reservoir on the lower substrate, as shown in Figure 16. This reservoir prevents the adhesive from flowing onto the substrate support components. Alternatively, a release agent may be applied to the parts that may come into contact with the adhesive. Figure 17 shows a butt joint manufactured using the proposed jig.

Figure 16. Silicone reservoir positioned on the lower substrate.

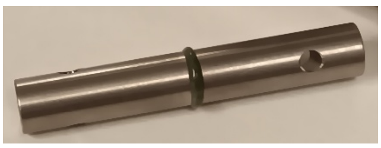

Figure 17. Final butt joint (with excess adhesive not removed).

The jig was primarily developed for cylindrical specimens with a diameter of 12.7 mm and a length of 40 mm (specimens in accordance with ASTM D2094). However, specimens with other dimensions can also be used. The diameter may vary between 8.5 and 14.5 mm. With regard to the length of the upper substrates, there are, in principle, no limitations. The jig also does not restrict the length of the lower substrates. In the case of substrates with a diameter smaller than 12.7 mm, it is not necessary to remove the base of the jig, as holes in the base allow the substrates to pass through. However, it is necessary to remove the base of the lower support, which serves as support for the lower substrate, and to raise the jig base relative to the workbench surface. In addition, the base of the jig can be removed and the jig can be used in a horizontal configuration, i.e., the vertical plate is positioned horizontally. In this case, there are no restrictions on the length of the lower substrate. The jig also enables the use of substrates with alternative cross-sectional geometries, such as square sections, provided they are correctly positioned on the V-shaped surfaces of the substrate supports.

Table 2 presents the cost of the main components, and it can be observed that the total cost of this jig was approximately €2100. A total of 90 substrates were also manufactured at an overall cost of €1080 (30 made of CK45 steel, 30 of AISI 304 stainless steel, and 30 of AW6082 aluminium).

Table 2. Indicative cost of the jig for butt-joint manufacturing at the time of manufacture.

Component	Quantity	Cost (nº of Pieces × Unit Cost)
Vertical Plate	2	2 × €120 = €240
Support pin	12	12 × €10 = €120
Support with V-shaped groove	12	12 × €50 = €600
Clamping jaw	6	6 × €40 = €240
Support clamping jaw	6	6 × €30 = €180
Handle (Elesa M.443-140-CH)	2	2 × €15 = €30
Base	2	2 × €110 = €220
Lateral plate	24	24 × €0.2 = €4.80
Support for lower adherent	6	6 × €25 = €150
Lower clamping jaws	6	6 × €40 = €240
Support bar (rear of the vertical plate)	6	6 × €2.43 = €14.58
Transverse steel bar	2	2 × €30 = €60
ISO 4762 M8×20 bolt	6	**
ISO 4762 M4×10 bolt	12	**
ISO 4762 M4×16 bolt	12	**
ISO 4762 M5×10 bolt	12	**
ISO 4762 M5×30 bolt	12	**
ISO 4762 M6×16 bolt	4	**
Total	86	€2099.38

** price is irrelevant, considering the remaining components.

2.3. Design and Manufacture of an Apparatus for Butt Joint Testing in a Tensile Testing Machine

For the execution of the tensile tests on the butt-joints, it was necessary to develop a dedicated apparatus for securing and loading the specimens. This apparatus is shown in Figure 18 (excluding the pins), and Table 3 presents a detailed list of its components, their cost, and respective functions. The total cost of this apparatus is approximately €650.

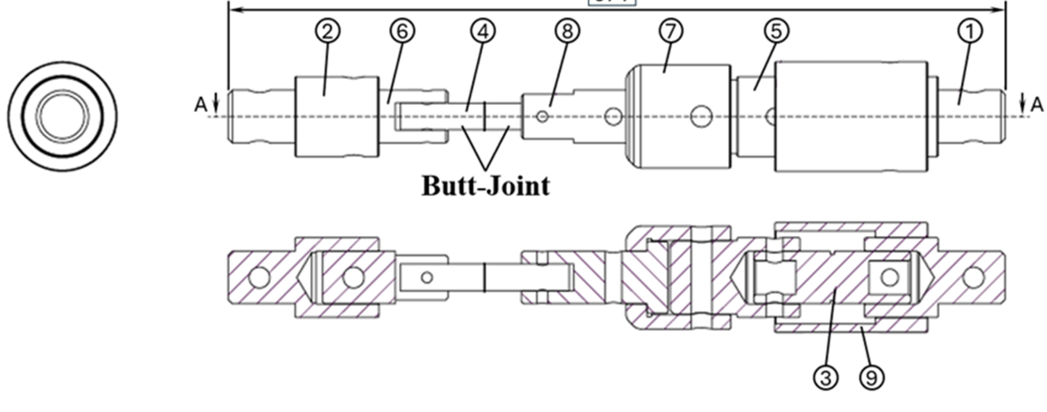

Figure 18. Representation of the apparatus for securing the butt joint in the tensile testing machine.

Table 3. Indicative bill of materials and manufacturing cost for the apparatus used to fix butt joints in the tensile testing machine.

Component and Cost	Description	Function/Remarks
1 (€65)	Lower support for securing the apparatus to the base of the tensile testing machine.	Provides stable attachment and alignment of the apparatus during testing.
2 (€65)	Upper support for attaching the apparatus to the load cell mounted on the movable crosshead of the tensile testing machine.	Transfers applied load from the crosshead to the specimen.
3 (€100)	Cardan joint.	Allows rotation and accommodates angular misalignment between connected components.
4	Butt-joint specimen (is not part of the apparatus).	The test specimen subjected to tensile loading.
5 (€65)	Cylindrical connecting piece linking the cardan joint to the components that secure the lower substrate of the butt joint.	Ensures load transmission from the cardan joint to the lower substrate support.
6 (€95)	Upper support for securing the upper substrate of the butt-joint via a 5 mm diameter pin.	Holds the upper substrate in position; the pin ensures proper alignment of the substrate hole.
7 (€80)	Hollow cylinder housing the upper portion of component (5) and the lower portion of the upper support (8).	Provides support and stability, allowing controlled movement and positioning.
8 (€95)	Lower support for securing the lower substrate of the butt-joint via a 5 mm diameter pin.	This component can rotate around its longitudinal axis to align the support hole with the substrate hole; holds lower substrate securely.
9 (€85)	Hollow cylinder housing the cardan joint and preventing component (5) from tipping after specimen failure or when no butt-joint is installed in supports (6) and (8).	Ensures safety and stability of the assembly during testing and after specimen rupture.

The numbering of the components is consistent with Figures 18 and 19. Figure 19 shows the individual manufactured components, while Figure 20 presents the fully assembled apparatus mounted on the tensile testing machine. Assembly of the components and attachment of the apparatus to the machine are achieved using pins. Both the upper and lower supports (Figure 19, components 6 and 8) are connected to cardan joints. A cardan joint is integrated into the apparatus for the lower support (Figure 19, component 3), while the tensile testing machine provides a second cardan joint for the upper support, connected to the load cell (Figure 20). This configuration allows accommodation of angular misalignments and promotes axial load transfer during testing.

Figure 19. Components of the apparatus for fixing butt joints.

During the fabrication of the butt-joints, the orientation of the substrate hole axes may be adjusted, typically to 0° or 90°, as illustrated in Figure 21. These holes accommodate the pins that secure the joint to the apparatus and transmit the applied tensile load. The developed jig described in the previous subsection allows precise control of this orientation. Additionally, the present testing setup enables testing of specimens with arbitrary hole orientations, as the lower support (Figure 19, component 8) can rotate about its longitudinal axis.

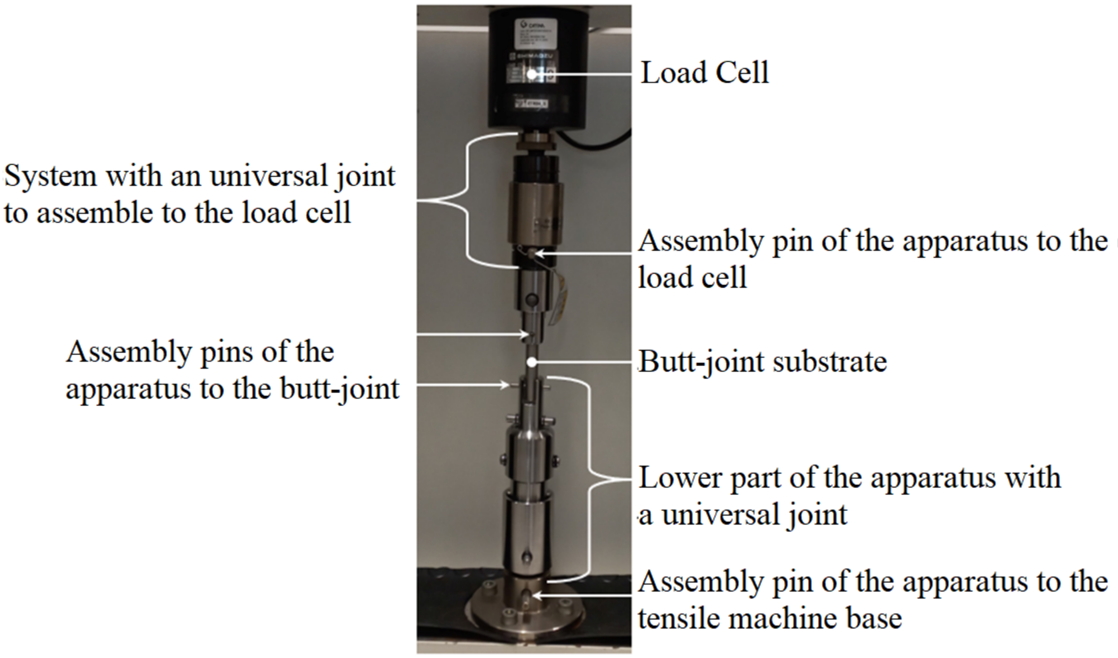

Figure 20. Apparatus for performing butt joint tests, fixed to the tensile testing machine.

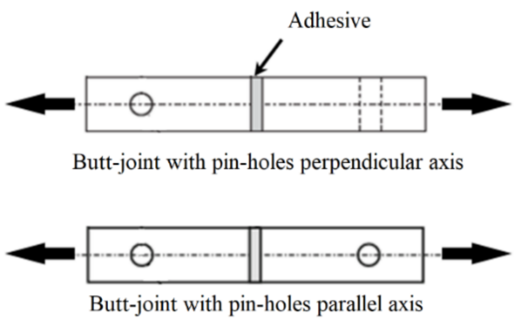

Figure 21. Orientation of the axes of pre-existing holes in the butt joint substrates.

The assembly of the apparatus and mounting of the specimen involve positioning and securing the lower and upper parts of the device to the testing machine, followed by insertion of pins to connect the specimen to the supports. Alignment between the support holes and the substrate holes is achieved through controlled adjustment of the crosshead position and rotation of the lower support. A small preload (approximately 10 N) is applied prior to testing to eliminate slack in the load path and ensure stable initial conditions.

All components comprising the tensile testing apparatus for cylindrical butt-joints were manufactured by machining from FR3 steel (DIN: 34CrNiMo6). As previously mentioned, the total production cost of the apparatus was approximately €650, with a detailed breakdown of the manufacturing costs for each component provided in Table 3.

It should be noted that all reported cost values are indicative and correspond to the conditions prevailing at the time of manufacture and procurement of materials and components. These values are therefore intended to provide an order-of-magnitude estimate and a relative comparison of the manufacturing effort associated with the different devices, rather than universal or time-invariant economic benchmarks.

3. Results and Discussion

The present work demonstrates that the systematic mechanical design of dedicated fixtures is a decisive factor in ensuring the reliability, repeatability, and standard compliance of adhesive joint testing. The floating roller peel fixture, the butt-joint fabrication jig, and the tensile testing apparatus were conceived as an integrated toolchain rather than as isolated devices, allowing specimen manufacture and mechanical loading to be treated as coupled stages within a single experimental system. This systems-based approach is particularly relevant in adhesive testing, where deviations in geometry, alignment, or boundary conditions can significantly alter the effective stress state within the joint.

From a manufacturing perspective, the developed fixture successfully combines structural rigidity with controlled kinematics. The floating roller fixture incorporates a bearing-supported roller arrangement and calibrated spacer rings that establish a 0.8 mm non-contact clearance between the roller ends and the side plates, thereby minimising parasitic friction and contributing to a stable peel path, which addresses one of the principal sources of uncertainty in peel testing. Although ASTM D3167 [31] prescribes the general testing principle, it does not define these detailed anti-friction and alignment-control solutions, which therefore represent the main original contribution of the present apparatus from a mechanical design perspective. The choice of bearing-supported rollers, combined with accurately machined shafts and lateral plates, promotes smooth motion governed predominantly by the applied load, rather than by fixture resistance. This design is consistent with the requirements of ASTM D3167 [31] standard and supports reproducible peel force measurements.

The butt-joint fabrication jig addresses a critical and often underreported source of experimental scatter: the control of adhesive layer thickness and substrate alignment during specimen preparation. The modular vertical-plate architecture, adjustable upper supports, and interchangeable mechanical stops enable fine control of the interfacial gap while maintaining concentricity of cylindrical substrates. The open geometry of the jig further allows full access to the bonding perimeter, facilitating surface preparation and excess adhesive removal. The decision to employ two smaller jigs rather than a single larger unit proved advantageous in terms of ergonomics, handling, and thermal management during elevated-temperature curing. The jig developed for the manufacture of butt joints satisfies the following requirements:

Ensures proper alignment of the substrates.

Allows adjustment of the adhesive thickness.

Enables the use of adhesives with different viscosities (liquids or pastes).

Provides access to the entire perimeter of the bonding area for removal of excess adhesive (in this case, the use of screws as stops is more suitable).

Allows adhesive curing at room temperature as well as at elevated temperatures, since the jig is manufactured from metallic materials (aluminium alloy and steel). However, for elevated temperatures, it is necessary to remove the handle and the rubber supports from the jig.

Enables the fabrication of up to six butt joints using cylindrical substrates with dimensions according to ASTM D2094, although substrates with other dimensions can also be used.

Is easy to handle (each jig weighs 7.75 kg). The handle also facilitates handling and transportation of the jig.

However, some disadvantages of the developed jig can also be identified when compared with jigs used for the same purpose. In fact, the developed jig is more complex, as it comprises a larger number of components and is likely more expensive. Furthermore, it includes components manufactured from different materials and, therefore, with different coefficients of thermal expansion, which, in the case of curing under elevated temperature, may introduce stresses both in the jig components and in the joint itself.

The tensile testing apparatus for butt-joints complements the fabrication jig by ensuring controlled load introduction during testing. The integration of cardan joints at both ends of the load path provides the necessary degrees of freedom for self-alignment, thereby reducing the risk of misalignment-induced bending. The possibility of rotating the lower support to accommodate different orientations of substrate holes further extends the versatility of the system. Together, these features address a fundamental limitation of many conventional tensile fixtures, namely the inability to fully decouple axial loading from secondary bending moments.

The indicative cost comparison shows that the primary investment lies in the butt-joint fabrication jig and associated substrates, reflecting the complexity of the alignment and thickness-control mechanisms. Nevertheless, these indicative costs suggest that the proposed devices may offer a practical balance between manufacturing effort and the benefits of improved experimental repeatability, reduced specimen rejection, and enhanced compliance with ASTM standards. The use of conventional machining processes and commercially available components further supports the transferability of the proposed designs to other laboratories.

It should be noted that the functional performance of the developed devices was experimentally validated, and the corresponding results are presented in a companion study [33]. In brief, the developed devices enabled the stable mechanical testing of adhesive joints manufactured with adhesives of distinct mechanical behaviour, allowing the acquisition of representative peel and tensile responses under controlled conditions. A detailed analysis of the corresponding force-displacement behaviour, strength values, and failure characteristics is provided in the companion study [33]. The referenced publication presents the experimental validation of devices designed for floating roller peel tests and tensile butt-joint tests, with the aim of enabling reliable mechanical characterisation of structural adhesives. The performance of the developed peel test fixture, as well as the jig and the apparatus for tensile testing, was evaluated using three commercially relevant adhesives: two epoxy systems (Araldite® AV 138 and Araldite® 420 A/B) and one polyurethane adhesive (SikaForce® 710).

4. Conclusions

This study presents the design and manufacture of a coherent set of mechanical devices for the experimental characterisation of adhesives and adhesively bonded joints, including a floating roller peel fixture, a butt-joint fabrication jig, and a custom tensile testing apparatus for butt joints. The developed devices were conceived in accordance with ASTM D3167, ASTM D897, and ASTM D2095 and were guided by core machine-design principles of alignment accuracy, controlled kinematics, structural rigidity, and manufacturing practicality.

The floating roller fixture provides a low-friction, mechanically stable solution for peel testing, while the fabrication jig enables accurate and repeatable control of adhesive thickness and substrate alignment. The tensile apparatus ensures controlled axial loading through self-aligning features that mitigate misalignment-induced bending. Together, these devices form an integrated experimental platform that enhances the reliability and reproducibility of adhesive joint testing.

The proposed designs demonstrate that careful mechanical engineering of testing tools is not merely an auxiliary concern, but a central component of experimental adhesive mechanics. By documenting the design rationale, manufacturing routes, and cost structure of the developed devices, this work contributes to the establishment of transparent and reproducible methodologies for adhesive testing and supports the development of more robust and reproducible experimental datasets for model validation and structural design.

Author Contributions

Conceptualisation: A.G.P., R.M.F. and P.J.R.O.N.; methodology: A.G.P. and P.J.R.O.N.; validation: A.G.P. and P.J.R.O.N.; formal analysis: A.F.V.P.; investigation: J.G.F.B., D.A.M.S. and I.M.P.; data curation: A.F.V.P. and A.G.P.; writing—original draft preparation: A.F.V.P., J.G.F.B., D.A.M.S. and I.M.P.; writing—review and editing: A.F.V.P., I.M.P. and A.G.P.; visualisation: A.G.P. and I.M.P.; supervision: A.G.P. and P.J.R.O.N.; project administration: A.G.P. All authors have read and agreed to the published version of the manuscript.

Funding

All costs associated with the devices developed in this work and the substrates were fully covered by a partner company (Gislotica–Mechanical Solutions).

Data Availability Statement

No new data was created.

Conflicts of Interest

The authors declare no conflict of interest.

Use of AI and AI-Assisted Technologies

During the preparation of this work, the author(s) used Grammarly Premium v6.8.263 to verify and improve the British (UK English) language employed. After using this tool/service, the author(s) reviewed and edited the content as needed and take(s) full responsibility for the content of the published article.

Appendix A

Original Design Features of the Developed Floating Roller Peel Apparatus Relative to ASTM D3167 Requirements

Although ASTM D3167 [31] defines the general testing principle and the functional configuration of the floating roller peel test, it does not prescribe in detail the specific mechanical solutions required to minimise parasitic effects such as friction, misalignment, or unintended contact between rotating and fixed components. In this context, the floating roller peel apparatus developed in the present work incorporates several original engineering features intended to improve the mechanical reliability and practical implementation of the test. Attention was given to the reduction of rotational resistance using a bearing-supported roller arrangement, comprising two rollers mounted on precision-machined shafts and supported by four SKF 61800 bearings. In addition, spacer rings were introduced to provide a controlled clearance of 0.8 mm between the roller ends and the lateral plates, thereby preventing parasitic contact and reducing frictional interference during testing. The apparatus also adopts a symmetric dual-side-plate configuration, which contributes to improved shaft alignment and helps preserve a stable peel path throughout the test. These features were selected to enhance the mechanical consistency of the fixture while maintaining a relatively simple and low-cost construction suitable for laboratory use. Table A1 summarises the principal original design features of the developed floating roller peel apparatus in relation to the functional requirements of ASTM D3167 [31], together with their expected mechanical effects.

Table A1. Original engineering features of the developed floating roller peel apparatus in relation to the functional requirements of ASTM D3167 [31].

ASTM D3167 Functional Requirement	Developed Engineering Solution	Quantitative/ Descriptive Value	Expected Mechanical Effect
Floating-roller peel configuration	Dual-roller assembly with bearing-supported rotation	2 rollers; 4 SKF 61800 bearings	Reduces rotational resistance during peeling.
Stable roller guidance and alignment	Symmetrical dual-side-plate layout with matched mounting holes	2 lateral plates, 3 mm thickness each	Improves shaft parallelism and preserves a stable peel path.
Minimisation of parasitic contact between rotating and fixed parts	Spacer rings inserted between roller ends and side plates	0.8 mm clearance	Prevents unintended contact and associated frictional interference.
Reliable transmission of motion through the roller assembly	Precision-machined shafts with stepped geometry fitted to the bearings and rollers	Shaft sections of 8, 10 and 12 mm diameter	Promotes concentric rotation and mechanical stability.
Structural robustness for repeated laboratory use	Machined steel construction with black oxide protection on most components	FR3 steel shafts; CK45 steel remaining parts	Enhances stiffness, durability, and dimensional stability.
Practical laboratory implementation	In-house manufacture using conventional machining and standard components	Indicative manufacturing cost ≈ €400	Provides a low-cost alternative to commercial systems.

References

1. Russo, M.; Zhang, D.; Liu, X.-J.; et al. A review of parallel kinematic machine tools: Design, modeling, and applications. *Int. J. Mach. Tools Manuf.* **2024**, *196*, 104118. https://doi.org/10.1016/j.ijmachtools.2024.104118.
2. Wei, Y.; Jin, X.; Luo, Q.; et al. Adhesively bonded joints—A review on design, manufacturing, experiments, modeling and challenges. *Compos. Part B Eng.* **2024**, *276*, 111225. https://doi.org/10.1016/j.compositesb.2024.111225.
3. Correia, D.S.; Costa, I.D.; Simões, B.D.; et al. Development of a Unified Specimen for Adhesive Characterisation—Part 1: Numerical Study on the Mode I (mDCB) and II (ELS) Fracture Components. *Materials* **2023**, *16*, 2951.
4. Pragathi, P.; Jenison, S.J.; Singh, G.R.; et al. Performance of adhesively bonded similar and dissimilar joints under cyclic hygrothermal aging for aerospace applications. *Int. J. Adhes. Adhes.* **2025**, *142*, 104130. https://doi.org/10.1016/j.ijadhadh.2025.104130.
5. Kupski, J.; Teixeira de Freitas, S. Design of adhesively bonded lap joints with laminated CFRP adherends: Review, challenges and new opportunities for aerospace structures. *Compos. Struct.* **2021**, *268*, 113923. https://doi.org/10.1016/j.compstruct.2021.113923.
6. Ciardiello, R.; Boursier Niutta, C.; Goglio, L. Adhesive Thickness and Ageing Effects on the Mechanical Behaviour of Similar and Dissimilar Single Lap Joints Used in the Automotive Industry. *Processes* **2023**, *11*, 433.
7. Rahmani, R.; Saeidi Googarchin, H. Adhesive bonding in impact crushing of automotive Al-CFRP hybrid tubes: A theoretical, experimental and numerical investigation. *Int. J. Adhes. Adhes.* **2025**, *142*, 104112. https://doi.org/10.1016/j.ijadhadh.2025.104112.
8. Lamberti, M.; Maurel-Pantel, A.; Lebon, F. Accelerated aging procedure of epoxy structural adhesive for marine offshore applications. *J. Adv. Join. Process.* **2024**, *9*, 100216. https://doi.org/10.1016/j.jajp.2024.100216.
9. Gude, M.; Meschut, G.; Flügge, W.; et al. Corrosion of adhesively bonded alloys in maritime environments: A review. *Int. J. Adhes. Adhes.* **2026**, *147*, 104264. https://doi.org/10.1016/j.ijadhadh.2026.104264.
10. Shu, Y.; Qiang, X.; Jiang, X.; et al. Durability of epoxy adhesives employed in civil engineering under hot/wet environments. *J. Build. Eng.* **2025**, *104*, 112366. https://doi.org/10.1016/j.jobe.2025.112366.
11. Machalická, K.V.; Vokáč, M.; Milerová, A.; et al. Improving water resistance of acrylate adhesive joints through atmospheric plasma treatment for civil engineering applications. *Prog. Org. Coat.* **2026**, *215*, 110101. https://doi.org/10.1016/j.porgcoat.2026.110101.
12. Romano, M.G.; Guida, M.; Marulo, F.; et al. Characterization of Adhesives Bonding in Aircraft Structures. *Materials* **2020**, *13*, 4816.
13. Dachev, D.; Kazilas, M.; Alfano, G.; et al. Towards Reliable Adhesive Bonding: A Comprehensive Review of Mechanisms, Defects, and Design Considerations. *Materials* **2025**, *18*, 2724.

14. Monajati, L.; Vadean, A.; Boukhili, R. Mechanical Behavior of Adhesively Bonded Joints Under Tensile Loading: A Synthetic Review of Configurations, Modeling, and Design Considerations. *Materials* **2025**, *18*, 3557.
15. Gu, Z.; Liu, Y.; Hughes, D.J.; et al. A parametric study of adhesive bonded joints with composite material using black-box and grey-box machine learning methods: Deep neuron networks and genetic programming. *Compos. Part B Eng.* **2021**, *217*, 108894. https://doi.org/10.1016/j.compositesb.2021.108894.
16. Tserpes, K.; Barroso-Caro, A.; Carraro, P.A.; et al. A review on failure theories and simulation models for adhesive joints. *J. Adhes.* **2022**, *98*, 1855–1915. https://doi.org/10.1080/00218464.2021.1941903.
17. Venkatappagari, S.; Mutra, R.R.; Mallikarjuna Reddy, D. State-of-the-art in adhesive joint technology: A comprehensive review of recent progress. *J. Mater. Res. Technol.* **2025**, *37*, 2593–2615. https://doi.org/10.1016/j.jmrt.2025.06.166.
18. Neves, L.F.R.; Campilho, R.D.S.G.; Sánchez-Arce, I.J.; et al. Numerical Modelling and Validation of Mixed-Mode Fracture Tests to Adhesive Joints Using J-Integral Concepts. *Processes* **2022**, *10*, 2730.
19. Fiedler, F.; Ehrenstein, J.; Höltgen, C.; et al. Jigs and Fixtures in Production: A Systematic Literature Review. *J. Manuf. Syst.* **2024**, *72*, 373–405. https://doi.org/10.1016/j.jmsy.2023.10.006.
20. Ibrahim, A.D.; Hussein, H.M.A.; Ahmed, I.; et al. Computer-Aided Design of Traditional Jigs and Fixtures. *Appl. Sci.* **2022**, *12*, 3.
21. ASTM International. *Standard Test Method for Tensile Properties of Adhesive Bonds*; ASTM D 897-08; ASTM International: West Conshohocken, PA, USA, 2015.
22. Van Massenhove, K.; Vandepitte, D.; Debruyne, S. Strength and stiffness variability study of viscoelastic adhesive butt joints. *J. Adhes.* **2019**, *95*, 350–368. https://doi.org/10.1080/00218464.2018.1563545.
23. Zhang, J.; Jia, H.; Li, H.; et al. Investigation on the uniaxial ratchetting and fatigue failure behaviors of silicone seal adhesive bonded butt-joints under tensile and torsional cyclic loading. *Int. J. Adhes. Adhes.* **2020**, *99*, 102588. https://doi.org/10.1016/j.ijadhadh.2020.102588.
24. Mu, W.-L.; Xu, Q.-H.; Na, J.-X.; Wang, H.; Tan, W.; Li, D.-F. Influence of temperature and humidity on the fatigue behaviour of adhesively bonded CFRP/aluminium alloy joints. *J. Adhes.* **2022**, *98*, 1358–1376. https://doi.org/10.1080/00218464.2021.1896362.
25. Wahab, M.M.A.; Hilmy, I.; Ashcroft, I.A.; Crocombe, A.D. Damage Parameters of Adhesive Joints with General Triaxiality Part I: Finite Element Analysis. *J. Adhes. Sci. Technol.* **2011**, *25*, 903–923. https://doi.org/10.1163/016942410X534939.
26. Möhring, H.-C.; Biermann, D.; Bleicher, F.; et al. Fixtures and workpiece clamping systems in machining. *CIRP Ann.* **2025**, *74*, 945–969. https://doi.org/10.1016/j.cirp.2025.04.096.
27. dos Reis, M.Q.; Marques, E.A.S.; Carbas, R.J.C.; et al. Functionally graded adherends in adhesive joints: An overview. *J. Adv. Join. Process.* **2020**, *2*, 100033. https://doi.org/10.1016/j.jajp.2020.100033.
28. Polini, W.; Corrado, A. Effects of adherends' misalignment on the 3-point flexural strength of single lap bonded joints. *Procedia CIRP* **2022**, *114*, 165–170. https://doi.org/10.1016/j.procir.2022.10.037.
29. Bartlett, M.D.; Case, S.W.; Kinloch, A.J.; et al. Peel tests for quantifying adhesion and toughness: A review. *Prog. Mater. Sci.* **2023**, *137*, 101086. https://doi.org/10.1016/j.pmatsci.2023.101086.
30. Akhavan-Safar, A.; Marques, E.A.S.; Carbas, R.J.C.; et al. 6—Stress analysis of adhesive joints. In *Adhesive Bonding*, 2nd ed.; Adams, R.D., Ed.; Woodhead Publishing: Cambridge, UK, 2021; pp. 159–192.
31. ASTM International. *Standard Test Method for Floating Roller Peel Resistance of Adhesives*; ASTM D 3167-10; ASTM International: West Conshohocken, PA, USA, 2010.
32. ASTM International. *Standard Test Method for Tensile Strength of Adhesives by Means of Bar and Rod Specimens*; ASTM D 2095-96; ASTM International: West Conshohocken, PA, USA, 2015.
33. Pedroso, A.F.V.; Campilho, R.D.S.G.; Pinto, A.G.; et al. A Comprehensive Evaluation of Peel and Tensile Strength in Adhesive Bonding. *J. Mech. Eng. Manuf.* **2026**, *in press*.